Ti, in each case at the totally excluded volume. Fraction 6 shows the highest Ti concentration (~ 0.2 ppm).

The elution of Fe species commences at the totally excluded volume for each SESC fraction. This is not the case with Cu and Zn, for which molecules of "size" smaller than an n-C_{35} alkane are predicted to elute.

Major Cu and Zn peaks eluting from fraction 1 correspond to ~ 1.3 ppm (Cu) and 0.4 ppm (Zn). The Cu metallogram from fraction 7 has relatively sharp peaks from which concentration can be estimated: progressing to smaller "sized" species (increasing elution volume), the concentrations are ~ 0.8, 2.3, and 1.1 ppm, respectively. Since fraction 7 is reputed to be polyphenols, these Cu signals may be due to the elution of Cu phenolates.

The Zn metallogram from fraction 7 exhibits the largest number of discrete peaks, four. The largest "sized" Zn compound elutes at the totally excluded volume and is ~ 6 ppm. Elution of the species at 10.5 ml indicates a molecule at the "size" of n-decane.

Fraction 8 has a Zn concentration of ~ 45 ppm, all of which elutes in a narrow band at the "size" of n-C_{24} alkane.

Fraction 9 displays a bimodal separation of totally excluded and selectively permeated (~ 0.25 ppm) Zn-containing matter.

As far as we know, we are the first to report distributions of organically bound metals in coal-derived products. The isolation of metal-organic fractions is a first step toward their speciation, which could yield information significant for both producing and utilizing coal liquids. Evidence for the survival of organometallic combinations of biological origin may be useful to geochemists concerned with the chemistry of coalification.

The source of organically bound metals in coal-derived materials is still uncertain. They may be present in the raw coal. They may be produced as a result of chemical reaction during the coal conversion process. They may originate with the processing equipment; we have observed large Cr concentrations in the process solvent used for the production of the SRC studied.

LARRY T. TAYLOR
DOUGLAS W. HAUSLER*
Department of Chemistry, Virginia Polytechnic Institute and State University, Blacksburg 24061
ARTHUR M. SQUIRES
Department of Chemical Engineering, Virginia Polytechnic Institute and State University

References and Notes

1. H. J. Gluskoter, *Adv. Chem. Ser.* **141**, 1 (1975); P. Zubovic, *ibid.* **55**, 221 (1966).
2. D. W. Hausler and L. T. Taylor, *Anal. Chem.* **53**, 1227 (1981).
3. The SRC was produced in a pilot plant at Wilsonville, Ala., operated by the U.S. Department of Energy and the Electric Power Research Institute. The coal was from the Amax mine in the Wyodak seam, near Gillette, Wyo. Conversion of organic matter in the coal to SRC was 85 to 90 percent. For a flow sheet of the SRC process, see D. D. Whitehurst, T. A. Mitchell, and M. Farcasiu [*Coal Liquefaction* (Academic Press, New York, 1980), p. 348].
4. We have also measured quantitatively a variety of trace elements in both pyridine and toluene extracts of the chloroform solubles in the Amax SRC, in distillables from this SRC, in an SRC process solvent, and in tars from coal gasification.
5. R. R. Ruch *et al.*, *Environ Geol. Notes Ill. State Geol. Surv. No.* 72 (1974).
6. L. Horton and K. V. Aubrey, *J. Soc. Chem. Ind. London* **50**, 541 (1950).
7. W. M. Coleman, P. Szabo, D. L. Wooton, H. C. Dorn, L. T. Taylor, *Fuel* **56**, 195 (1977).
8. W. M. Coleman, P. Perfett, H. C. Dorn, L. T. Taylor, *ibid.* **57**, 612 (1978).
9. D. W. Hausler, J. W. Hellgeth, L. T. Taylor, J. Borst, W. B. Cooley, *ibid.* **60**, 40 (1981).
10. V. A. Fassel and R. N. Kniseley, *Anal. Chem.* **46**, 1110A (1974); *ibid.*, p. 1155A.
11. M. Farcasiu, *Fuel* **56**, 9 (1977).
12. We used a μ-Styragel column (Waters Associates, Milford, Mass.). Molecules of large effective molecular size are not retained by a size exclusion column and therefore elute first at the totally excluded volume.
13. D. W. Hausler, J. W. Hellgeth, H. M. NcNair, L. T. Taylor, *J. Chromatogr. Sci.* **17**, 617 (1979).
14. Supported by the Commonwealth of Virginia and the Department of Energy under grant EF-77-01-2696. We thank E. Denyszyn for technical assistance in preparing the metallograms for publication.
* Present address: Research and Development Laboratory, Phillips Petroleum Company, Bartlesville, Okla.

18 November 1980; revised 4 May 1981

Polycrystalline Echinoderm Calcite and Its Fracture Mechanics

Abstract. *Polycrystalline calcite was revealed by scanning electron microscopy of fractured skeletal ossicles of the sea star* Echinaster spinulosus *(Echinodermata, Asteroidea). Whisker-like calcite crystals were observed in specimens that were loaded in stress relaxation before being fractured; rapidly broken surfaces were smooth and glassy. The crystallites were 1300 angstroms wide and at least 3600 angstroms long and were packed together in lamellae. The lamellae were wound into spirals that formed the trabecular bars. All the crystallites in an ossicle appear to be aligned in the same direction. Geometric considerations indicate that the requirement for packing the crystallites smoothly may explain the high magnesium ion concentration of echinoderm calcite.*

Virtually all echinoderms have an endoskeleton composed of calcite ossicles or spicules. As a skeletal material, echinoderm calcite has several unusual features: (i) macroscopically, the calcite forms a fenestrated structure of trabeculae pierced by roundish holes (stereom); (ii) the calcite is "impure," containing 4 to 16 percent Mg^{2+} substituted for Ca^{2+} (*1*); (iii) evidence for an organic matrix within the calcite is equivocal (*2*); and (iv) each skeletal element, excepting echinoid teeth, behaves optically as a single crystal (*3, 4*). It is not clear whether each skeletal element (spine, plate, or ossicle) is monocrystalline or an aggregation of crystallites with perfectly aligned optical axes. X-ray crystallographic analyses indicate that each skeletal element could be referred to a single crystal lattice (*4*). Although the data did not rule out a polycrystalline substructure (*5, 6*), the perfect alignment of crystallites required to explain the x-ray data had seemed unlikely. Furthermore, since extensive scanning electron microscopy of fractured skeletal surfaces had failed to reveal a polycrystalline substructure (*3–5*), most workers preferred the monocrystalline hypothesis (*3–5, 7, 8*).

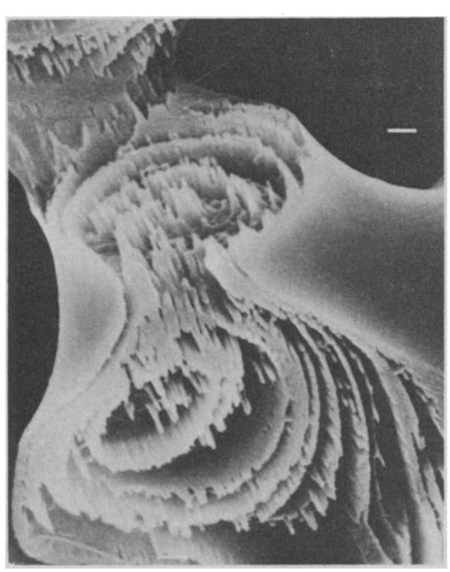

Fig. 1. Scanning electron micrograph of a fractured trabecular bar within a skeletal ossicle of the sea star *E. spinulosus*. Whisker-like calcite crystallites aligned in spiral lamellae demonstrate the polycrystalline substructure of the calcite ossicle. Scale bar, 10 μm; magnification, ×5000.

I now present evidence that the skeletal elements of echinoderm calcite are polycrystalline. Carinal and dorsolateral ossicles of the sea star *Echinaster spinulosus* (Asteroidea: Spinulosida) were fractured during mechanical tensile testing of strips of the aboral body wall of the ray. Scanning electron micrographs of the fractured ossicle surfaces indicate that the skeletal ossicles of *E. spinulosus* are polycrystalline aggregates (Figs. 1 and 2). Needle-like crystallites are packed together in lamellae that form concentric circular or spiral courses. The lamellae are probably part of a continuous sheet, rolled up in a spiral, since in many instances such a spiral course can be followed around the central axis (Figs. 1 and 2B, arrow). The width of the lamellae is about 2000 ± 200 Å (mean ± standard error, $N = 24$) (*9*). Most of the concentric surfaces of the lamellae are smooth, with tiny grainy irregularities, and resemble the smooth external surface of the trabecula. Some of the surfaces show striations that look like cleavage lines.

The individual crystallites resemble slender needles or whiskers (Figs. 1 and 2, B and D). They are parallel to each other, and their long axes are parallel to the central axis of the spiral (deviations average less than 1°, $N = 134$) (*10*). Individual crystallites protruding from the trabecular fracture surfaces (Fig. 2, C and D) are about 1300 ± 100 Å on a side ($N = 48$). Because one end was concealed it was not possible to measure their length; but they extend an average of 3600 ± 250 Å ($N = 47$) above the surrounding area. The tips of the crystallites are similar to scalenohedral calcite crystals, although they are too small for face angles to be measured. Face angles were measured on a few larger crystallites in the center of some scanning electron micrographs (for example, the centers of Fig. 2, C and D), in which one face appeared to be parallel to the front of the camera (*10*). These angles averaged 74° ± 1° ($N = 21$), which approximates the characteristic rhombohedral cleavage angle of calcite, 74°, 55′ (*11*). The crystallites appear to be closely aligned calcite crystals composed of about 200 cleavage rhomb-unit cells (*12*) on their short faces; their length is at least three times their width.

The parallel crystallite orientation is retained in the three-dimensional structure of the stereom. A single trabecular bar may contain more than one central axis (Fig. 1). Extensions and branches perpendicular to the axial direction are built up by many layers of lamellae in which the crystallite length is shortened. Gradually curved struts are produced because the crystallites are quite small. This pattern is visible where large continuous trabecular surfaces have fractured (Fig. 2B, upper right, and C, right).

The precise orientation of the crystallite axes with respect to the anatomical axes could not be determined because of distortion of the specimen as it fractured. However, the long axis of the crystallites, and hence the central axes of the spirals, lay close to the transverse axis of the ray. I observed no evidence of an organic matrix between the lamellae or crystallites, although such material might be difficult to discern in scanning electron micrographs. It is unlikely that organic material was removed during preparation of the specimens (*13*).

The polycrystalline structure was apparent only in specimens that were loaded in stress relaxation before they were fractured (*14*). Intact strips (*15*) of the dorsal body wall were loaded in tension along the longitudinal, transverse, or oblique ray axes, or in torsion about the longitudinal axis until fracture (*14*). When specimens were loaded and broken rapidly (elongations of about 0.01 percent per second) in any of the above ways, ossicle fractures with the smooth conchoidal surfaces typical of echinoderm calcite were always produced (*3, 7, 8*) (Fig. 2A). These smooth fractures occurred across the narrow portions of trabecular bars. The tightly packed crystallite whiskers were apparently stressed in a manner that prohibited fracture along calcite cleavage planes during fast fracture.

Crystallites were detected in all specimens that had been stress-relaxed before being fractured, regardless of the direction in which the load was applied. The calcite crystallites cleaved freely along their rhombohedral planes. Trabeculae fractured across the entire area surrounding the holes (Fig. 2, B and C); at areas of high curvature (Fig. 2C), surface flaws characteristic of stress concentration developed. Ossicle fracture was generally confined to areas near the junction of ossicles and dermis; collagen fibers tended to shred away from the stereom.

Under stress relaxation, the junction between collagen and calcite was probably altered, causing the calcite to lose its characteristic strength properties and allowing the crystallites to cleave. The nature of this alteration is unknown.

Other evidence suggests that polycrystalline skeletal ossicles are not restricted to *E. spinulosus*, nor even to Asteroidea.

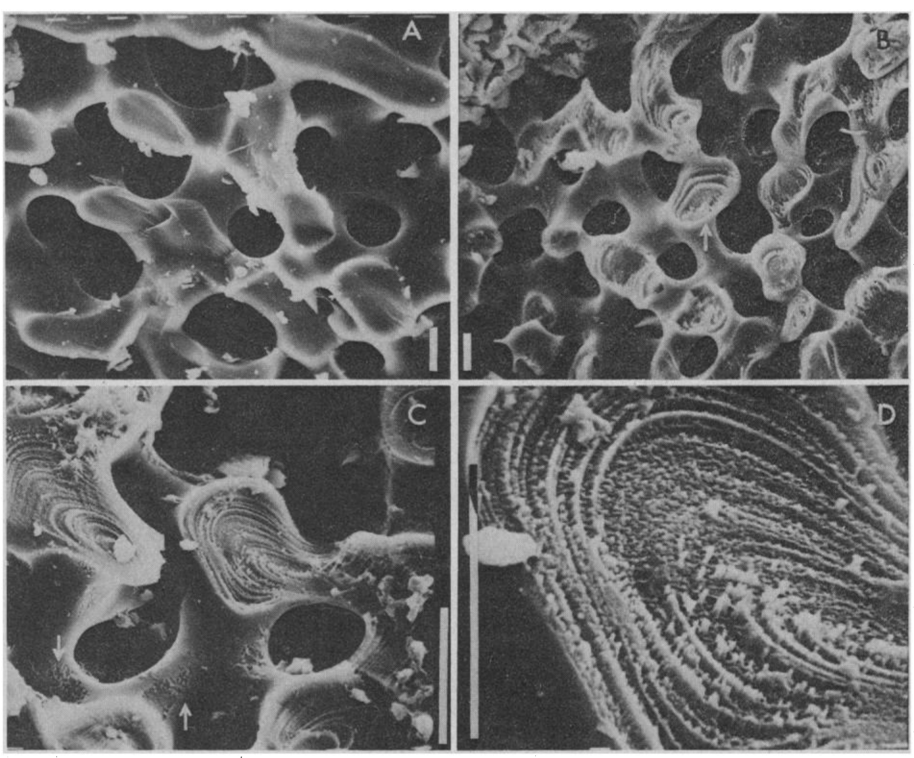

Fig. 2. Scanning electron micrographs of fracture surfaces of skeletal ossicle of *E. spinulosus*. Scale bars, 10 μm. (A) Smooth fractures produced by rapid breaks. The glassy fracture surfaces are characteristic of echinoderm calcite (×1500). (B) Fracture surface produced after stress-relaxation. The lamellae of crystallites follow a spiral course (arrow). Layers of lamellae stack up to produce branches and struts. The flaky material at the upper left is collagen (×1000). (C) Spiral lamellae and stress concentration flaws (arrows) on the normally smooth trabecular surface. The long axes of the crystallites all point in the same direction despite the plane of fracture. (D) Individual crystallites that protrude from the surface are roughly rhombohedral. Pointed tips, however, may be scalenohedral (×7500).

Puzzling laminar (*3*) or "zonar" structures (*5*) resembling the concentric lamellae that I observed have been seen in scanning electron micrographs of fractured echinoid plates. A scanning electron micrograph of a broken trabecular bar from a young urchin (*16*) shows jagged structures that resemble crystallites, and Pearse and Pearse (*16*) suggest that organic material might be contained between lamellae. Theoretical (*17*) and x-ray diffraction (*18*) evidence also indicate polycrystallinity.

Some of the enigmatic features of echinoderm calcite can be explained if the polycrystalline model is typical of echinoderms. Crystallite lamellae may contribute to the strength of the stereom in two ways. (i) The crystallites are whisker-like and may share some of the strength properties (*19*) of whisker crystals. (ii) Since the outer trabecular surfaces are tightly packed cleavage faces, they are extremely smooth. The surface perfection of the trabeculae may produce strengthening by crack inhibition (*3*, *7*, *8*). The *Echinaster* material demonstrated loss of this surface smoothness at areas where stress concentrations were likely (Fig. 2C, arrows).

The curvature of the lamellae may explain the high Mg^{2+} concentration of echinoderm calcite. A smooth, curved surface cannot be formed from calcite crystals, which are rhombohedral, because the outer circumference must be greater than the inner circumference. The ionic radius of Mg^{2+} (0.67 Å) (*12*) is 32 percent smaller than that of Ca^{2+} (0.98 Å) (*12*), and magnesian calcites have smaller interplanar spacings in the crystal lattice (*20*). If the magnesium ions are located within the crystallites so that the inner faces are slightly contracted, the crystallites would fit together smoothly. Where the curvature is greatest—around tight curves and near the central axis—Mg^{2+} would be more abundant than in the straighter sections of lamellae. Overall Mg^{2+} content varies among the different skeletal elements (*6*), but it is not known whether Mg^{2+} content varies with any of the smaller structural features such as lamellae.

All echinoderm ossicles are bound by connective tissue of some sort (*21*). Since the ossicle-dermis junction appears to be sensitive to loading rate, failure to observe crystallites in other studies may have been the result of producing fractures by rapid compression.

PATRICIA L. O'NEILL*
Department of Zoology,
Duke University,
Durham, North Carolina 27706

References and Notes

1. K. E. Chave, *J. Geol* **62**, 266 (1952).
2. L. Klein and J. D. Currey, *Science* **169**, 1209 (1970).
3. D. Nichols and J. D. Currey, in *Cell Structure and Its Interpretation*, S. M. McGee-Russell and K. F. A. Ross, Eds. (Arnold, London, 1968), pp. 251–261.
4. G. Donnay and D. L. Pawson, *Science* **166**, 1147 (1969).
5. H.-U. Nissen, *ibid.*, p. 1150.
6. D. M. Raup, in *Physiology of Echinodermata*, R. A. Boolootian, Ed. (Wiley, New York, 1966), pp. 379–395.
7. J. D. Currey, in *Mechanical Design in Organisms*, S. A. Wainwright *et al.*, Eds. (Wiley, New York, 1976), p. 218.
8. D. Nichols, *Echinoderms* (Hutchinson, London, 1969), pp. 123–125.
9. Measurements were taken from the scanning electron micrograph negatives, 75 by 95 mm, which were magnified (×5) with a photographic enlarger. Linear measurements were taken from the image with vernier calipers to the nearest 0.1 mm; measurements could be repeated within ± 10 percent (N = 50). Since it was not possible to correct for perspective, the measurements are approximate.
10. Angular measurements, taken from enlarged negatives (*9*), were read by use of a protractor with a vernier scale to the nearest 0.1° and rounded to the nearest degree. Care was taken to minimize perspective and parallax, although error is unavoidable in measuring a three-dimensional object in two dimensions. Angular measurements could be repeated within 0.8° (N = 25).
11. E. S. Dana and W. E. Ford, *Dana's Manual of Mineralogy* (Wiley, New York, ed. 16, 1952), p. 265.
12. W. A. Deer, R. A. Howie, J. Zussaman, *Rock-Forming Minerals*, vol. 5, *Non-Silicates* (Wiley, New York, 1962), pp. 227–255.
13. All scanning electron microscopy specimens were fractured during mechanical testing (*14*). Those not immediately prepared for microscopy were stored in buffered 10 percent Formalin. Specimens were dipped in distilled water to remove sea salts, then air-dried under cover for 1 week. They were then coated with 200 Å of gold-palladium and examined with a JEOL scanning electron microscope.
14. Test sections were cut from the dorsal body wall of a sea star; the ossicles were loaded indirectly by pulling on the collagenous portion of the body wall. For fast fractures, the sea star was unanesthetized. The specimens were clamped into a mechanical testing machine with two rubber-padded screw clamps. One clamp was attached to a fixed carriage and the other to a sliding carriage with braided wire and binding posts. The position of the sliding carriage was adjusted with a thumbscrew that allowed the specimen to be stretched and fractured. Displacement was monitored by two colinear linear variable differential transformers whose cores were attached to the specimen by two needle points. Force output was delivered by a strain gauge on a cantilever fixed to the stationary carriage mount. Force and displacement were recorded on a Brush dual-pen recorder. Fast fracture specimens were loaded in tension at an elongation rate of about 1 percent per second until fracture. The specimens were irrigated with artificial seawater (Instant Ocean) during testing. For stress relaxation, the sea stars were anesthetized in 0.1 percent MS-222 in artificial seawater for 1 hour before the test sections were cut. The sections were irrigated with the same solution during the experiment. The MS-222 was necessary to prevent muscle contraction, which deformed the specimen, although no differences in fracture surfaces were apparent in stress-relaxed specimens that were not treated with MS-222. The specimens were placed in the mechanical testing machine and loaded in tension at 3 to 8 MN/m^2. Force was continuously recorded; when the force had decayed to near 0, usually after about 10^3 seconds, the specimen was pulled at an elongation rate of about 1 percent per second until it was fractured.
15. The ossicles lie within a collagenous dermis to which they are firmly attached by collagen fibers that project through holes in the stereom.
16. J. S. Pearse and V. B. Pearse, *Am. Zool.* **15**, 731 (1975).
17. K. M. Towe, *Science* **157**, 1048 (1967).
18. H. U. Nissen, *Neues Jahrb. Geol. Palaeontol. Abh.* **117**, 230 (1963).
19. S. S. Brenner, in *Fiber Composite Materials* (American Society for Metals, Metals Park, Ohio, 1965), pp. 11–36.
20. J. R. Goldsmith, D. L. Graf, O. I. Joensuu, *Geochim. Cosmochim. Acta* **7**, 212 (1955).
21. L. H. Hyman, *The Invertebrates*, vol. 4, *Echinodermata* (McGraw-Hill, New York, 1955), p. 4.
22. I thank S. Wainwright for his assistance, enthusiasm, and encouragement during this study. J. Hebrank designed and built the mechanical testing machine, which I modified for use in this work. Supported by research funding and a postdoctoral fellowship from the Cocos Foundation, Inc.
Present address: Department of Biology, Portland State University, Box 751, Portland, Ore. 97207.

18 December 1980; revised 22 April 1981

Quiet Zone Within a Seismic Gap near Western Nicaragua: Possible Location of a Future Large Earthquake

Abstract. *A 5700-square-kilometer quiet zone occurs in the midst of the locations of more than 4000 earthquakes off the Pacific coast of Nicaragua. The region is indicated by the seismic gap technique to be a likely location for an earthquake of magnitude larger than 7. The quiet zone has existed since at least 1950; the last large earthquake originating from this area occurred in 1898 and was of magnitude 7.5. A rough estimate indicates that the magnitude of an earthquake rupturing the entire quiet zone could be as large as that of the 1898 event. It is not yet possible to forecast a time frame for the occurrence of such an earthquake in the quiet zone.*

Segments of seismically active plate boundaries in the circum-Pacific that have not been ruptured by a large (magnitude M greater than 7) earthquake for 30 years or more are considered likely locations for future large earthquakes (*1*, *2*). The earthquake potential of each segment, or "seismic gap," is considered to increase with the time since the last large earthquake within that segment. Since 1973, when this concept was presented by Kelleher *et al.* (*1*), nearly all large circum-Pacific earthquakes have occurred within such gaps. Thus the concept has been of great utility in forecasting where large earthquakes should occur. To be socially useful, however, earthquake predictions must specify the time of these events more accurately. Some workers (*3*) have reported precursory patterns of seismicity that may make possible the forecasting of large